Surface modes in metal–insulator composites with strong interaction of metal particles

Vladimir V. Lebedev · Sergey S. Vergeles ·
Petr E. Vorobev

Abstract We theoretically examine plasmonic resonance excited between two close metallic grains embedded into a dielectric matrix. The grains sizes are assumed to be much less than the wavelength of the electromagnetic wave in the dielectric medium and the grain's separation is assumed to be much smaller than the grains sizes. A qualitative scheme is developed that enables one to estimate frequency of the plasmonic resonance and value of the field enhancement inside the gap. Our general arguments are confirmed by rigorous analytic solution of the problem for simplest geometry—two identical spherical grains.

1 Introduction

Interaction of electromagnetic field with metallic grains whose dimensions are smaller than the wavelength is a subject of intensive experimental and theoretical interest for a long time [1, 2]. Convex metal surface creates the conditions for localized surface plasmon excitations, whose resonance frequencies are below plasma frequency in metal. The surface plasmon excitation can lead to a strong enhancement in both light scattering and absorbtion near the resonance frequency and is accompanied by a large value of the electric field near a particle or a system of particles [3].

V. V. Lebedev · S. S. Vergeles · P. E. Vorobev
Landau Institute for Theoretical Physics RAS, Kosygina 2,
Moscow 119334, Russia

V. V. Lebedev · S. S. Vergeles (✉) · P. E. Vorobev
Moscow Institute of Physics and Technology, Institutskij per. 9,
141700 Dolgoprudnyj, Moscow Region, Russia
e-mail: vergeles@gmail.com

Resent progress in nanofabrication has led to thriving activity in the actual design of subwavelength structures such as dimers [4–10] and arrays of metallic particles [11]. Optical properties of such objects are very different from those of separate particles. The strongest field enhancement occurs in gaps between closed metallic grains, scattering and absorbtion increase compared to those for single grains. The enhancement can reach sufficient values to observe Raman detecting of single molecule [12, 13] placed into the gap (see also [14] as a basic reading on SERS). The resonance frequency is shifted in the systems, it is observed experimentally [8, 7] and numerically [15–17] that the shift depends both on the polarization of the incident light and on the inter-particle distance in dimers or arrays. The red-shift of the resonance maximum is observed when the electric field of the incident wave is polarized along the axis of the dimer or array while the blue-shift happens when the electric field is perpendicular to the axis. The extent of the shift depends on the inter-particle distance and the particle size.

The shift of the resonances can be observed, in particular, in so-called semi-continues metallic films [18–20], see also [21]. The films are disordered systems which are metallic grains placed on a dielectric substrate, with broad distributions of sizes and/or inter-grain gap widths. The distribution leads to existence of surface plasmon excitations in the films for broad band of frequencies. Strong field enhancement occurs only in part of the gaps for given frequency of incident light, and the choice of the gaps changes with the frequency. As an alternative, one can find broad spectrum of surface plasmon frequencies in periodical systems [22] where selected range of eigen frequencies corresponds to Brillouin zone.

The most commonly used metals for manufacturing the grain systems are noble metals since their plasma

frequency lies in the ultraviolet region and imaginary part of the dielectric permittivity is small compared to the real one in the optical region [23]. It is known [24] that the plasmonic resonance in a single metallic grain is excited at a frequency near the plasma one lying near the ultraviolet spectral region for noble metals. To reach the resonance in the optical or near-infrared diapason, one should use a special geometry where metallic grains are separated by distances much smaller than their size. The resonance conditions imply, particularly, large negative dielectric permittivity of the grains [15].

Here, we theoretically investigate the phenomenon, considering particular case of two closed metallic grains. We establish that the resonance conditions are related mainly to the local geometrical characteristics of the gap. The field enhancement is more sensitive to geometrical factors controlling the energy flow to the gap. Our general arguments are confirmed by a rigorous analytical solutions. One can think about an extension of our results to periodic and disordered metal–dielectric composites.

Theoretical explanation of the observed effects is difficult due to the fact that even the system of two particles is too complicated for exact analytical approach. For monochromatic fields (which we are considering), the system of Maxwell's equations leads to Helmholtz equation for both electric and magnetic fields, which cannot be solved analytically for systems of two or more metallic particles. However, in the systems under consideration the particles sizes are of the order of tens of nanometers, which is smaller than the wavelength (hundreds of nanometers), and the quasi-stationary approach can be used. In this limit, the Helmholtz equation is reduced to Laplace equation which can be solved explicitly for a wider set of systems, and particularly for the system of two metallic particles. Namely one can separate variables in the so-called bi-spherical reference frame [25–31]. In the work [26], the problem of two spheres was approached in this way and the resonance conditions have been found, however, the field enhancement was not considered explicitly and some extraneous solution were presented as to be physical solutions. In this paper we utilize the same analytical approach and find both the resonance conditions and the field enhancement. In particular, we show the way how to exclude the extraneous solutions. We also present a simple qualitative explanation of the phenomenon allowing one to estimate the field values by the order of magnitude.

The structure of the paper is as follows. In Sect. 2, we give general theoretical relations enabling one to analyze the electromagnetic wave propagation through the metal–insulator composites and develop a scheme enabling one to estimate parameters of the giant field enhancement in the metallic dimer where grain's sizes a are much smaller than the wavelength in the dielectric matrix and the depth of the

skin layer in the metal and the grains are separated by a narrow gap of width $\delta, \delta \ll a$. Section 3 is devoted to a rigorous analytical investigation of the giant field enhancement in the system of two close metallic spherical grains. The obtained results confirm the estimates given in the previous section and enable to extract all the numerical factors for the particular geometry. Our main results are outlined in Sect. 8 where also perspectives and unsolved problems are discussed. Technical details of our calculations can be found in "Appendices". Some preliminary results of the work were already published, see Ref. [25]. The results concerning two close grains of cylindrical form were published in Ref. [32].

2 Basic relations

We consider the electromagnetic wave refraction on a metal–insulator composite that is a system of metallic grains embedded into a dielectric matrix. We consider monochromatic wave with frequency ω. The electric field strength is written as $\mathrm{Re}[\mathbf{E}\exp(-i\omega t)]$ where $\mathbf{E}(\mathbf{r})$ is a (complex) field amplitude to be investigated. We assume that both metal and dielectric have no magnetic properties at frequencies we examine, so that their permeability can be regarded to be equal to unity. Then the system is characterized by the electric permittivity $\varepsilon(\omega)$, which is the function of the frequency and is different in the dielectric matrix and in the metallic grains.

The electric permittivity of the dielectric $\varepsilon_\mathrm{d}(\omega)$ is assumed to be of the order of unity and to have negligible imaginary part. We accept a local relation between the electric field strength and the electric displacement field $\mathbf{D}, \mathbf{D} = \varepsilon_\mathrm{m}(\omega)\mathbf{E}$, in the metal grains. Here, ε_m is the electric permittivity of the metal. In optical and near-infrared spectral regions, the permittivity of a noble metal can be described by the Drude–Lorentz formula

$$\varepsilon_\mathrm{m} \sim -\frac{\omega_\mathrm{p}^2}{\omega^2 + i\omega/\tau}, \tag{1}$$

where ω_p is the plasma frequency and τ is the electron relaxation time. Therefore in the frequency interval $\omega_\mathrm{p} \gg \omega \gg \tau^{-1}$, the permittivity ε_m has negative real part, large by its absolute value, and relatively small imaginary part. The same is true for the dielectric contrast $\varepsilon = \varepsilon_\mathrm{m}/\varepsilon_\mathrm{d}$.

We examine the case where the metallic dimer (two close metallic grains) is surrounded by an unbounded dielectric medium. The grains are assumed to be small, that is, their sizes are much less than the wavelength $\lambda_\mathrm{d} = \lambda/\sqrt{\varepsilon_\mathrm{d}}$ of the electromagnetic wave in the surrounding dielectric medium and the depth of the skin layer in metal $\lambda/\sqrt{|\varepsilon_\mathrm{m}|}$, where λ in the wavelength in vacuum. We are

investigating the electromagnetic field profile near the dimer, especially in the gap between the grains, where one expects an essential enhancement of the field. The problem belongs to the so-called near-field optics. The electric field **E** near the small metallic grains can be examined in quasi-electrostatic approximation (see, e.g., Ref. [2]), in terms of its potential Φ, $\mathbf{E} = -\mathrm{grad}\,\Phi$. Then the potential Φ has to satisfy the equation

$$\mathrm{div}[\varepsilon(\mathbf{r})\,\mathrm{grad}\,\Phi] = 0, \tag{2}$$

formally coinciding with the electrostatic equation for the electric field potential in a non-homogeneous dielectric medium.

The electric permittivity is assumed to be homogeneous inside the grains and in the surrounding dielectric medium. Then Eq. (2) is reduced to the Laplace equation

$$\nabla^2 \Phi = 0, \tag{3}$$

in each of the regions. The Eq. (3) should be complemented by boundary conditions at the interface between the metal and the dielectric medium that are continuity of normal component of the electric displacement field and of the tangent components of the electric field. In terms of the electrical potential Φ, the conditions are reduced to continuity of the potential Φ and to the relation between its normal derivatives on different sides of the interface, their ratio should be equal to the dielectric permittivity contrast ε

$$\partial_n \Phi\big|_{\mathrm{d}} = \varepsilon \partial_n \Phi\big|_m. \tag{4}$$

We are interested in the electric field enhancement, characterized by the ratio E_c/E^{ext}, where E_c is the electric field strength in the central segment of the gap between the grains, and E^{ext} is the electric field strength in the incident electromagnetic wave. An essential enhancement has to be observed near resonance frequencies, then there are two principal contributions to the ratio,

$$E_c/E^{\mathrm{ext}} = G/(\varepsilon - \varepsilon_{\mathrm{res}}) + G_{\mathrm{bg}}, \tag{5}$$

that can be called resonance and background terms. Expression (5) follows from the general properties of Maxwell equations when all materials have linear electric response. The quantity $\varepsilon_{\mathrm{res}}$, as well as the factors G and G_{bg}, are determined by geometry of the grains and by the gap thickness. A maximum value of the enhancement is observed at the resonance, $\varepsilon' = \varepsilon_{\mathrm{res}}$, then $|E_c/E^{\mathrm{ext}}| \approx G/\varepsilon''$, where ε' and ε'' are real and imaginary parts of the dielectric contrast ε (both are functions of frequency). Thus, the electric field enhancement is restricted by energy losses. The resonance frequency can be evaluated now from expression (1), $\omega_{\mathrm{res}} \sim \omega_{\mathrm{p}}/\sqrt{|\varepsilon_{\mathrm{res}}|}$.

Pure real value of $\varepsilon_{\mathrm{res}}$ in (5) implies that energy losses are determined primarily by the Ohmic dissipation in the metal grains. Besides, the charge oscillations in the dimer lead to radiation of the energy from the dimer. This radiation diminishes the field enhancement and can be phenomenologically accounted by inclusion of negative imaginary correction into $\varepsilon_{\mathrm{res}}$. Then, the electric field enhancement at resonance is $|E_c/E^{\mathrm{ext}}| \approx G/(\varepsilon'' - \varepsilon_{\mathrm{res}}'')$.

2.1 Qualitative description

Let us present a qualitative description of the electromagnetic field enhancement for a dimer consisting of two close metallic grains. We assume that the gap width δ between the grains is much smaller than the curvature radius a of the grains near the gap, $\delta \ll a$. We assume also that a is a characteristic grain size. An example of such system is depicted in Fig. 1a where two identical spheres of radii a separated by a narrow gap are presented. Below, we present an analytical solution for the spheres. Here, we give a qualitative picture for two arbitrary grains with smooth boundaries.

Plasmon resonance modes of a single remote spherical metallic grain were found and classified in Refs. [24, 33]. It was shown there, that modes of a small metallic grain with a radius a less than wavelength correspond to n-pole oscillations of the charge in the metal. Resonant frequencies of the oscillations are determined by the condition

$$\varepsilon_{\mathrm{res}} = -1 - 1/n, \tag{6}$$

determining the resonant dielectric contrast ε. The value $n = 1$ corresponds to dipole modes, then $\varepsilon_{\mathrm{res}} = -2$. The relation (6) gives the resonant frequencies close to the plasma frequency of the (bulk) metal (provided the dielectric constant of the dielectric medium is of order unity).

The dimer constituted of two remote metallic grains was considered in Ref. [34]. Then the eigen modes of the grains couple weakly that leads to shifting the resonant frequencies of the dimer in comparison with a single grain. In the particular case of two identical metallic spherical grains, the resonance condition characterizing the coupled dipole
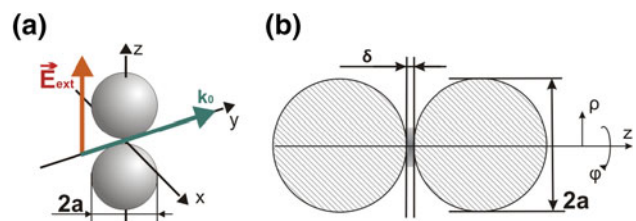

Fig. 1 **a** 3D view of two metallic identical spherical grains, $\boldsymbol{k}_0$ is the wavenumber of the incident light. **b** The cross section of two metallic identical spherical grains; the intensity of the electric field achieves its maximum value in the area between the grains, which is marked as *dark*

mode having axial symmetry with respect to OZ axis becomes

$$\varepsilon = -2\left(1 \pm a^3/\delta^3\right). \tag{7}$$

As before, δ is the distance between the grains, however, here it is assumed to be much greater than the grain dimension, $\delta \gg a$. The sign 'plus' corresponds to the symmetric mode in regard to middle plane which separates the grains whereas the sign 'minus' corresponds to the antisymmetric one. In recent work [35], the technics of coupled modes was used for analytic investigation of the problem. However, the technics does not match for analytical investigation of the limit of close grains: one should keep large number of harmonics to catch the physics. The fact can be checked with the help of numerical simulation using the expansion, see e.g., Ref. [34]. This is the reason why the results [35] are not compatible neither with our results nor with previous results [26].

Let us stress that we analyze the opposite limit of close grains where the field distribution in space has nothing in common with slightly disturbed eigen modes of separate grains. In our case, the electric field of the resonance mode is localized in the central segment of the gap between the grains where the gap can be regarded as approximately flat (grey region in Fig. 1b). In the limit the only 'symmetric' mode is relevant. The resonance value of the dielectric contrast for the mode shifts toward large negative values $|\varepsilon| \gg 1$, whereas Eq. (7) gives only small corrections to the value $\varepsilon = -2$.

It is instructive to use results of Ref. [36] for the electromagnetic field propagation in the metal–dielectric–metal structures to establish properties of the electric field distribution in the flat region. The electromagnetic wave can propagate along a narrow flat gap between two metallic bodies separated by a dielectric medium provided $\varepsilon = -\coth(\beta\delta/2)$ where β is the propagation constant and δ is the gap width. We are interested in the case $|\varepsilon| \gg 1$, then the above relation is reduced to $\beta = -2/(\varepsilon\delta)$. For our system of grains, we anticipate that the plasmon resonance arises when a standing wave is excited in the flat segment of the gap between the grains. The standing waves are determined by the conditions $\beta h \approx \pi n$ where n is an integer number and h is the longitudinal size of the gap. The size of the flat region between the grains can be estimated as $h \sim \sqrt{a\delta}$ for spherical grains. Thus, we obtain the following estimation for the resonance values of the permittivity contrast

$$\varepsilon_{\text{res}} \sim \frac{h/\delta}{n} \sim -\frac{\sqrt{a/\delta}}{n}, \tag{8}$$

where the integer number n numerates different modes. The second evaluation in (8) is given for the case of spherical grains. The estimation is valid provided $n \ll h/\delta$

that ensures the condition $\beta\delta \ll 1$ (it is equivalent to the inequality $|\varepsilon| \gg 1$).

Let us describe the spatial structure of the principal resonant plasmon mode, corresponding to $n = 1$. Due to excitation of the mode, surface charges appear on grains. Some charges of opposite signs are concentrated on the grain surfaces in the flat region, at distances smaller than h from the gap center, like in the flat capacitor. The electric field is approximately homogeneous in the flat region of the gap between the grains. Since each grain is uncharged, some compensatory charges are distributed at distances larger than h from the gap center. The dielectric contrast ε is effectively infinite at the distances, since the inverse surface plasmon propagation constant is much greater than the separation from the gap center ρ in the region. Thus, the problem of electric field distribution is reduced to an electrostatic problem. Grain's surfaces are equipotential in the case and the potential difference $\Delta\Phi$ between grains is constant. That leads to the conclusion that both the surface charge density and the electric field behave $\propto 1/\rho^2$ at distances $h \ll \rho \ll a$, since the separation between the grains can be estimated as ρ^2/a there. Therefore, the dipole moment of the dimer is determined by the distances $\rho \sim a$, compare Ref. [37]. Thus,

$$E \sim d/(a\rho^2), \tag{9}$$

in the domain $h \ll \rho \ll a$. Since the grains are uncharged, the electric field flux through any closed surface surrounding one of the grain is zero. Applying the condition to the plane separating the grains, we obtain from Eq. (9)

$$E_c \sim \frac{d}{a^2\delta} \ln \frac{a}{\delta}, \tag{10}$$

where E_c is the electric field in the central part of the gap. The relation (10) means compensation of the field fluxes through the central (flat) region and the region $h < \rho < a$.

The enhancement factor G defined in (5) can be found by equating the Ohmic dissipation to the energy pumping produced by the external field. The solution for the plasmon waves in plane gap [36] shows that the penetration depth of the electric field is equal to the wavelength, which is h for our mode. Thus, the energy dissipation is concentrated in the grain regions of sizes h near the gap that leads to dissipation power

$$I_Q \sim \omega\varepsilon''(E_c/\varepsilon)^2(\sqrt{a\delta})^3, \tag{11}$$

where E_c/ε estimates the electric field inside the metal. The energy pumping at resonance can be estimated as $\omega d E^{\text{ext}}$. Equating the quantity to expression (11) one finds

$$\frac{E_c}{E^{\text{ext}}} = \frac{G}{\varepsilon''}, \quad G \sim \frac{(a/\delta)^{3/2}}{\ln(a/\delta)}, \tag{12}$$

where we exploited Eqs. (8) and (10). For frequencies different from the resonance, one should return to the general expression (5).

The dependence of the electric field enhancement factor G (12) on the resonance number n can be obtained from more careful investigation of the electric field spatial structure, which uses adiabatic approximation for quasi-planar gap. The theory of adiabatic approximation is developed in "Appendix 1". It is shown in the "Appendices" that the ratio (10) increases with the mode number, $E_c/d \propto n$. The evaluation (11) for Ohmic losses should be corrected due to the penetration depth for the field decreases as $1/n$, now the losses are $I_Q \sim \omega \varepsilon'' (E_c/\varepsilon)^2 h^3/n^2$. Finally, resonance value of dielectric contrast $\varepsilon_{\mathrm{res}}$ scales as $1/n$, see (8). Thus, the enhancement factor G obtains additional factor $1/n$ for modes with $n > 1$.

Quasi-static approximation we use is valid until the radiation becomes comparable with the Ohmic losses inside the metallic grains. The radiation intensity I_ω is determined by far asymptotics of the electric field at $\rho \gg a$, and thus, by dipole moment d of the system, $I_\omega \sim \omega d^2/\lambda_d^3$, where $\lambda_d = \lambda/\sqrt{\varepsilon_d}$ is the wavelength in the surrounding dielectric media. Thus, the criteria $I_Q \gg I_\omega$ is necessary for validity of (12) based on pure quasi-static approximation. Assuming that the dielectric constant ratio $\varepsilon \sim \sqrt{a/\delta}$, the criteria can be rewritten in the form

$$(a/\lambda_d)^3 \ll \frac{\varepsilon_m''}{\varepsilon_m} \ln^2(a/\delta). \tag{13}$$

If the Ohmic losses in the metal are relatively small, the condition is not satisfied and the main part of losses stems from the radiation. The enhancement factor at the resonance is

$$\frac{E_c}{E^{\mathrm{ext}}} \sim \frac{\lambda_d^3}{a^2 \delta} \ln(a/\delta) \tag{14}$$

in the limit. The enhancement factor (14) grows with the mode number as n. Hence, the Ohmic dissipation becomes the main source of the losses in the system at large n, and the estimation (12) is valid for the limit.

Here, we note that the applicability criteria for resonance frequencies (8) is $\lambda_d^2 \gg h^3/\delta$, which follows from the requirement that the wavelength of the plasmon wave in the gap should be less than the depth of the skin layer in metal. For spherical grains, the condition is equivalent to $(a/\lambda_d)^3 \ll \lambda_d/\delta$, thus it is weaker than (13). Hence, both limits (12, 14) may take place when the resonance condition is still determined by (8).

3 Two identical spherical grains

Here, we analytically examine the case of two close identical spherical metallic grains of radii a separated by a narrow gap of width δ, $\delta \ll a$, see Fig. 1b. Let us introduce the reference system where the axis Z goes through the centers of the metallic balls and the $X-Y$ plane is the symmetry plane of the system. Then the grain surfaces are determined by the equation

$$\rho^2 + [z \pm (a + \delta/2)]^2 = a^2, \tag{15}$$

where $\rho^2 = x^2 + y^2$.

It is useful to pass into the bispherical coordinate system (see, e.g., Ref. [38, pp.301–303]) with the coordinates ξ, η, φ where φ is the polar angle and other two variables are defined using the relations

$$\rho = \frac{a \sinh \xi_0 \sin \eta}{\cosh \xi - \cos \eta}, \quad z = \frac{a \sinh \xi_0 \sinh \xi}{\cosh \xi - \cos \eta}, \tag{16}$$

where ξ_0 is a constant. There are two reasons for introducing the reference system. First, the Laplace equation (3) is separated in terms of the variables ξ, η, φ. The corresponding system of eigen modes of the Laplace equation can be found in Ref. [38]. Second, the equation (15) for the grain surfaces is rewritten as $\xi = \pm \xi_0$ for a particular choice of the constant ξ_0 satisfying $\sinh^2(\xi_0/2) = \delta/(4a)$, that is implied below. For close grains, where $\delta \ll a$, the parameter ξ_0 is small and the above relation leads to $\xi_0 = \sqrt{\delta/a}$.

The variable ξ runs from $-\infty$ to $+\infty$. The region $\xi < -\xi_0$ corresponds to the 'lower' grain interior ($z < 0$), the region $\xi > \xi_0$ corresponds to the 'upper' grain interior ($z > 0$), and the region $-\xi_0 < \xi < \xi_0$ corresponds to the dielectric medium. The variable η is defined in the domain $0 < \eta < \pi$. When η runs from 0 to π (at constant ξ, φ), a curve is drown starting and finishing at the axis Z inside or outside the grains (depending on the value of ξ). The starting and the finishing points are different, therefore, Φ is not periodic in η whereas it is periodic in φ.

In our investigation, we can partly rely on the results obtained for the electrostatic case. The electrostatic field around two dielectric balls, placed into an external homogeneous electric field is examined analytically in Ref. [31]. The case of two touched dielectric balls was investigated numerically in Ref. [39]. The electrostatic field around two spherical metallic grains, placed into an external homogeneous electric field is discussed in Ref. [37], where recurrence relations were obtained for the expansion coefficients of the potential Φ over eigen functions of the Laplace equation. The limit of two close metallic balls was analyzed separately in Ref. [40]. There are also some results for the electromagnetic field that can be compared with our conclusions. Two metallic balls placed into an incident plane electromagnetic wave were considered in the works [29, 30], where the recurrence relations were obtained and then solved numerically for different parameters. Similar

results were obtained in Ref. [41]. Finally, in Ref. [26], the recurrence relations were obtained and the resonance values for contrast of dielectric permittivities were found.

3.1 Recurrence relations

The grain closeness means that only 'symmetric' plasmon modes are of interest, see Ref. [36]. The electric potential in such modes is antisymmetric, $\Phi(z) = -\Phi(z)$ or $\Phi(\xi) = -\Phi(-\xi)$. Correspondingly, we assume that the electric field of the incident electromagnetic wave is polarized along the Z axis. For an arbitrary case, the electric field strength E^{ext} of the incident wave near the dimer should be simply substituted by the z-component of the strength.

For our case of grains smaller than the wavelength of the incident electromagnetic wave, its potential can be approximated as by a linear function of coordinates near the grains. Thus, the electric field potential of the incident wave is

$$\Phi^{\text{ext}} = -E^{\text{ext}}z = -E^{\text{ext}}a\frac{\sinh\xi_0\sinh\xi}{\cosh\xi - \cos\eta}. \tag{17}$$

It can be represented as an expansion over eigen functions of the Laplace equation in the bispherical reference system

$$\Phi^{\text{ext}} = \sum_{n=0}^{\infty} \Phi_{\alpha}^{\text{ext}}\phi_{\alpha,0-}(\xi, \eta), \tag{18}$$

where the eigen functions are given by Eq. (41). The expansion (18) is correct in the region $\xi > 0$, to find the expansion in the region $\xi < 0$ one can use the relation $\Phi^{\text{ext}}(-\xi) = -\Phi^{\text{ext}}(\xi)$. The expansion coefficients $\Phi_{\alpha}^{\text{ext}}$ are

$$\Phi_{\alpha}^{\text{ext}} = -\sqrt{2}(2\alpha + 1)E^{\text{ext}}a\sinh\xi_0. \tag{19}$$

The expressions can be obtained using the generating function $(\cosh\xi - \mu)^{-1/2}$ of the Legendre polynomials, see [Eq. (14.7.19), 42].

The potential Φ outside the metal grains can be represented as a sum of the external potential Φ^{ext} and the induced potential $\Phi^{\text{ind,out}}$. The induced potential $\Phi^{\text{ind,out}}$ satisfies the Laplace equation (3), as well as Φ^{ext}, and can be, consequently, expanded over the same eigen functions

$$\Phi^{\text{ind,out}} = \sum_{\alpha \geq |m|}^{\infty} B_{\alpha}^{m}(\phi_{\alpha,m+} - \phi_{\alpha,m-}). \tag{20}$$

Note, that the expression is odd in z. Inside one of the grains, say, corresponding to $\xi > \xi_0$, the electric potential can be represented as

$$\Phi^{\text{in}} = \sum_{\alpha \geq |m|}^{\infty} A_{\alpha}^{m}\phi_{\alpha,m+}. \tag{21}$$

It is an expansion over functions satisfying the Laplace equation and analytical at $\xi \to \infty$.

Now, we use the boundary conditions. The continuity of the potential at the grain's boundaries leads to the following expression for the coefficients A_n^m

$$A_{\alpha}^{m} = \Phi_{\alpha}^{\text{ext}}\delta_{m0} + \left[e^{(2\alpha+1)\xi_0} - 1\right]B_{\alpha}^{m}, \tag{22}$$

where $\delta_{m\alpha}$ is the Kronecker symbol. The boundary condition (4) becomes

$$X_{\alpha,m}^{-}B_{\alpha-1}^{m} + X_{\alpha,m}B_{\alpha}^{m} + X_{\alpha,m}^{+}B_{\alpha+1}^{m} = D_{\alpha}\delta_{m0}. \tag{23}$$

Explicit expressions for the coefficients in the equation are written in "Appendix 2".

There is an additional condition imposed onto the expansion coefficients B_{α}^{m} that follows from the Laplace equation (3). Since both Φ and $\rho^{|m|}e^{-im\varphi}$ satisfy the Laplace equation, we find $\nabla[\nabla\Phi\rho^{|m|}e^{-im\varphi} - \Phi\nabla(\rho^{|m|}e^{-im\varphi})] = 0$. Integrating the relation over volume of one of the grains, and converting the integral to the surface one we arrive at the condition (it is useful to use [Eq. 2.17.4.5, 43] on the way)

$$\sum_{\alpha=|m|}^{\infty} \frac{(\alpha + |m|)!}{(\alpha - |m|)!}B_{\alpha} = 0. \tag{24}$$

The condition (24) at $m = 0$ means simply that the grains remain uncharged. The requirement removes some extraneous solutions, which were assigned in Ref. [26] to be really existing and are called T modes.

The system of the recurrence equations (23) resolves into independent systems of recurrence equations for different axial numbers m. General scheme of the solution for the recurrence equations is as follows: recurrence equations (23) allows one to express step-by-step B_{α}^{m} through $B_{|m|}^{m}$, and then the condition (24) fixes the value of $B_{|m|}^{m}$. After that, the coefficient A_{α}^{m} has to be found from Eq. (22). However, realization of the program needs an infinite number of steps. Nevertheless, one can obtain a set of analytical results for close spherical grains.

Note that only angular harmonics with $m = 0$ are excited by the external field in the main approximation in a/λ, since both the harmonics and the field of the incident wave have the same axial symmetry. That is why below we concentrate on the case $m = 0$.

3.2 Axially symmetric modes

Here, we consider axial symmetric solutions described by the modes with $m = 0$. We examine the case of close balls, then $\xi_0 \ll 1$. Expanding the coefficients in the recurrence equation (23), see Eqs. (42, 43), over ξ_0, one obtains (we omit the index $m = 0$ for brevity in the subsection)

$$X_\alpha^- = -\alpha \frac{\alpha_\varepsilon - (\alpha - 1)}{\alpha_\varepsilon + 1/2},$$

$$X_\alpha = (2\alpha + 1)\frac{\alpha_\varepsilon - \alpha}{\alpha_\varepsilon + 1/2},$$

$$X_\alpha^+ = -(\alpha + 1)\frac{\alpha_\varepsilon - (\alpha + 1)}{\alpha_\varepsilon + 1/2}, \qquad (25)$$

$$D_\alpha = \frac{\sqrt{2}aE^{\text{ext}}}{\alpha_\varepsilon + 1/2},$$

where α_ε is determined by the relation

$$\varepsilon = -\coth\left[\left(\alpha_\varepsilon + \tfrac{1}{2}\right)\xi_0\right]. \qquad (26)$$

Accounting for the inequality $|\varepsilon| \gg 1$ we obtain approximately $\alpha_\varepsilon \approx -1/(\xi_0\varepsilon) - 1/2$.

A partial solution of the Eq. (23) with the coefficients (25) is

$$B_\alpha^{\text{part}} = \frac{(2\alpha + 1)\xi_0}{\exp[(2\alpha + 1)\xi_0] - 1}\sqrt{2}aE^{\text{ext}}, \qquad (27)$$

see "Appendix 2". All factors in the expression are positive. Consequently, the partial solution cannot satisfy the condition (24) that is reduced to $\sum B_\alpha = 0$ for $m = 0$. Therefore, one should add to the partial solution a solution of the homogeneous equation B_α^{hom} that is simply $B_\alpha^{\text{hom}} = (\alpha - \alpha_\varepsilon)^{-1}$, provided $\xi_0\,\alpha \ll 1$. The other linear independent solution decays too slowly at large α, see Eqs. (46) and (48), and thus, the second solution cannot be used to satisfy the condition (24). We arrive at the conclusion that the solution of the Eq. (23) is $B_\alpha = B_\alpha^{\text{part}} + \zeta B_\alpha^{\text{hom}}$, the factor ζ should be determined from the condition $\sum B_\alpha = 0$.

One can find the factor ζ near the resonance frequencies that are determined by eigen modes of the homogeneous equation (23) (without the right hand side). To find resonance values of α_ε or ε, one should substitute into the condition $\sum B_\alpha = 0$ the solution $B_\alpha^{\text{hom}} = (\alpha - \alpha_\varepsilon)^{-1}$. Then summation over α should be cut at $\alpha \sim 1/\xi_0$, since at larger α the solution B_α^{hom} starts to decay exponentially, see (48). As a result, we find

$$\sum_{\alpha = 0}^{[\alpha_\varepsilon]} \frac{1}{\alpha_\varepsilon - \alpha} = \sum_{[\alpha_\varepsilon]+1}^{\xi_0^{-1}} \frac{1}{\alpha - \alpha_\varepsilon}, \qquad (28)$$

where $[\alpha_\varepsilon]$ means the integer part of α_ε. The solutions of the equations are positive, $\alpha_\varepsilon > 0$. The solution which has the smallest value is

$$1/\alpha_\varepsilon \approx -\ln\xi_0 \Leftrightarrow \varepsilon\xi_0 = -2 - 4/\ln\xi_0, \qquad (29)$$

with the logarithmic accuracy. Other solutions of Eq. (28) can be represented as $\alpha_\varepsilon = \alpha_n$ where

$$\alpha_n = n - 1 - 1/\ln(n\xi_0), \qquad (30)$$

and n is an integer number satisfying the inequality $n \ll \xi_0^{-1}$. The solution (29) corresponds to $n = 1$. In terms of the dielectric contrast, the resonance condition (30) is rewritten as

$$\varepsilon_{\text{res}} = -\xi_0^{-1}[n - 1/2 - 1/\ln(\xi_0 n)]^{-1}, \qquad (31)$$

The resonance condition (31) is in accordance with our previous estimates (8) since $\xi_0 = \sqrt{\delta/a}$. The result (31) was obtained in [26] by the same manner.

If the dielectric contrast ε is close to the resonance value (31), then the main contribution into the sum $\sum B_\alpha^{\text{hom}}$ is determined by the deviation of B_α^{hom} from its resonance value. The sum $\sum B_\alpha^{\text{part}}$ can be found explicitly using the expression (27). Then, we obtain from the relation $\sum(B_\alpha^{\text{part}} + \zeta B_\alpha^{\text{hom}}) = 0$ the following expression

$$\zeta = -\frac{\sqrt{2}\pi^2 aE^{\text{ext}}}{12\xi_0^2}\frac{(n - 1/2)^{-2}}{\left[\ln\left(n\xi_0\right)\right]^2}\frac{1}{\varepsilon - \varepsilon_{\text{res}}}. \qquad (32)$$

The applicability condition of the expression is $|1 - \varepsilon/\varepsilon_{\text{res}}| \ll n/|\ln(n\xi_0)|$.

3.3 Electric field profile

The expressions found above enable one to find the electric potential Φ in accordance with Eqs. (20, 21). We concentrate on a vicinity of the first resonance corresponding to $n = 1$ in the expressions (31, 32). The electric field is examined in the plane $z = 0$ where the potential is equal to zero. Therefore, we calculate the electric field there. Details of calculations can be found in "Appendix 2", here we present only the final results.

At distances $\rho \lesssim n\sqrt{a\delta}\ln(a/\delta)$ from the Z axis, the term with $\alpha = [\alpha_\varepsilon]$ in the sum (50) gives the leading contribution into the electric field. In particular, it coincides in the region with the electric field of two point charges of opposite signs, placed in singular point of the transformation (16) points $z = \pm a\sinh\xi_0$ for the first resonance. Thus,

$$E_z \approx -E^{\text{ext}}\frac{8\pi^2(a/\delta)^{3/2}}{3(2n - 1)\ln(a/\delta n^2)}\frac{1}{\varepsilon - \varepsilon_{\text{res}}}\frac{P_n(\mu)}{(1 + \rho^2/a\delta)^{3/2}}, \qquad (33)$$

where $\mu = \cos\eta$ and $P_n(\mu)$ is Legendre polynomial. For first resonance $n = 1$ the expression demonstrates that at $\rho \ll \sqrt{a\delta}$ the electric field is a constant that is in accordance with the expression (5) and the estimation (12). For higher resonance, expression (33) confirms our qualitative analysis, based on adiabatic approximation, see "Appendix 1".

As we argued in Sect. 2, there exists an intermediate domain of ρ where the potential difference between the

grain surfaces does not depend on ρ. Now we can formulate more accurately the lower boundary of the region, that is, $n\sqrt{a\delta}\ln(a/\delta)$. The electric field in the region, $n\sqrt{a\delta}\ln(a/\delta) \ll \rho \ll a$, is calculated in "Appendix 2":

$$E_z \approx E^{\text{ext}} \frac{16\pi^2}{3(2n-1)^2} \frac{\sqrt{a/\delta}}{\ln^2[a/\delta n^2]} \frac{1}{\varepsilon - \varepsilon_{\text{res}}} \frac{a^2}{\rho^2}, \tag{34}$$

and all terms in sum (50) having $\alpha \lesssim \rho/\sqrt{a\delta}$ give contribution to the electric field. Note that the electric field changes its sign at the boundary value $\rho \sim n\sqrt{a\delta}\ln(a/\delta)$. The charge density on the grain surfaces also changes its sign there. The expression (24) corresponds to the law (9).

As we already noted, near a resonant frequency, there are the resonant and the background contributions into the electric field E_c in the gap, see Eq. (5). Calculating the electric field in the center of the gap, one obtains for the nth resonance,

$$G = \frac{8\pi^2}{3(2n-1)} \frac{(a/\delta)^{3/2}}{\ln[a/\delta n^2]}, \quad G_{\text{bg}} = -2\sqrt{a/\delta}. \tag{35}$$

Note that the enhancement factor G diminishes as n grows. It is instructive to compare our results with the electrostatic case, when $\omega = 0$. The limit was investigated in Ref. [37]. Using the solution, one can obtain the field enhancement in the center of the gap between two conducting spherical grains

$$\frac{E_c}{E^{\text{ext}}} = \frac{2\pi^2}{3} \frac{a/\delta}{\ln(a/\delta)}. \tag{36}$$

The enhancement is parametrically weaker than our dynamic case.

At large distances, $\rho \gg a$, the induced electric field tends to the electric field of a point dipole, $E_z \approx -d/\rho^3$, where

$$d = -E^{\text{ext}} \frac{4\pi^4}{9} \frac{\sqrt{a/\delta}}{(2n-1)^2 \ln^2[a/\delta n^2]} \frac{a^3}{\varepsilon - \varepsilon_{\text{res}}}. \tag{37}$$

Note the extra logarithmic factor in the expression for the dipole moment d. The expression (37) being substituted into the formulae (9, 10) gives estimations corresponding to Eqs. (33, 34).

Finally, let us account for radiation losses, which can be included in all above formulae though negative imaginary part of ε_{res}. For the purpose, we assume Ohmic losses to be absent and resonance condition to be satisfied. For definiteness, we assume the phase of E^{ext} to be zero, then the dipole moment d is pure imaginary at the resonance. The energy pumping is $W = \omega E^{\text{ext}} \text{Im}[d]/2$ whereas the radiation losses are $I_\omega = 8\pi^3 \omega |d|^2/3\lambda_d^3$. Thus, the dipole moment $d = i(3/16\pi^3)\lambda_d^3 E^{\text{ext}}$. Comparing with (37), we conclude that

$$\varepsilon_{\text{res}}'' = -\frac{64\pi^7}{27} \frac{\sqrt{a/\delta}}{(2n-1)^2 \ln^2(a/\delta n^2)} \frac{a^3}{\lambda_d^3}. \tag{38}$$

4 Conclusion

Let us outline the main results of our work. We established that the frequency of the surface plasmon in the system of two close metallic grains of nanoscale size is determined by the geometrical characteristics of the gap and the frequency dependence of the dielectric constants of the metal and the surrounding media. It is convenient to express the resonance condition directly in terms of the contrast ε of dielectric constants of the metal and of the surrounding media. The contrast should be negative and large by its absolute value if the curvature radius of the gap a is much larger than its width δ. The estimate for the resonance contrast ε is given by Eq. (8), it is confirmed by the rigorous consideration for the spherical grains, see Eqs. (31). To find the resonance frequency ω, one should know a frequency dependence of the contrast $\varepsilon(\omega)$ which is determined mainly by the frequency dispersion of the metal dielectric constant $\varepsilon_m(\omega)$ for a given metal, if the dielectric permittivity of the surrounding media has weak dispersion of the dielectric constant. The resonance frequency is determined from the relation $\varepsilon'(\omega) = \varepsilon_{\text{res}}$. For rough estimations, one can use the Drude–Lorentz formula (1).

The question concerning the field amplification inside the gap is more subtle. General form for the frequency dependence of the amplification factor on the frequency near a resonance frequency can be written in the form (5). The amplification coefficient G is estimated differently for nearly spherical and nearly cylindrical grains, see the estimate (12) which is valid if the Ohmic losses dominate and the radiation losses are negligible for the system. The estimate is confirmed by rigorous solution of the problem for the spherical and cylindrical grains, see Eq. (35). One should use instead estimate (14) for the field enhancement factor in the opposite limit when the radiation losses are dominate. In terms of general relation (5), the losses can be accounted by adding positive imaginary part into the resonance dielectric contrast ε_{res}, see (38). We anticipate that for more sophisticated geometry (say, for close strongly prolate grains arranged along an axis) the amplification factor can be even larger than for the spherical grains. However, the problem needs an additional investigation.

In our analysis, we used the quasi-static approximation that implies that all the characteristic sizes of the grains are much less than the electromagnetic wavelength in the homogeneous dielectric medium and the skin layer depth in the metal. We established that the resonance mode is localized between the grains, at distances $\rho \lesssim \sqrt{a\delta}$ from the

gap center, where δ is the width of the gap and a is the curvature radius of the surface of the grains in the gap area. And just this small area determines the resonance condition (8). Therefore the condition survives provided the quasi-static approximation does work at the scale, that is if the scale $\sqrt{a\delta}$ is less than $\lambda/\sqrt{|\varepsilon_m|}$ where λ is the wave length in vacuum. That leads to the condition $\lambda^2/\varepsilon_d \gg a^{3/2}\delta^{1/2}$, justifying Eq. (8) even for large grains. However, the amplification factor in this case should be determined using complete geometry of the system and Maxwell equations.

Since the resonance mode is localized between the grains, a principal role in giant electric field enhancement for a random distribution of the grains is played by grain dimers with suitable separations, satisfying the resonance condition. Thus, a number of sharp peaks in the space distribution of the electric field has to be observed in the disordered metal–dielectric composite in the external electromagnetic wave. Experimental data [7, 10] qualitatively prove the conclusion, see, e.g., Refs. [44, 45]. To determine the number of peaks at a given frequency, one has to know a probability distribution of small separations δ (in comparison with the grain sizes) in grain dimers.

Recently considerable efforts are applied in designing periodic metal–dielectric composites, see, e.g., Ref. [46]. One could imagine a periodic structure of metallic grains (say, of metallic spheres) separated by small distances. In this case, resonance modes can be excited where the electric field has sharp maxima in central segments of the gaps between the grains. However, due to overlapping of the modes localized near the gaps, the resonance has to be transformed into a band of delocalized modes, like it occurs for electrons in a periodic potential (crystalline lattice). As our analysis shows, the structure of the electric field in the gap between the grains at distances smaller than the grain size is fixed by boundary conditions at the metal–dielectric interface. Therefore, the resonance frequency has to be determined by matching conditions in the regions between the grains, instead of the condition at infinity for two grains immersed in an unrestricted dielectric medium. Thus, we expect that the band width is of the order of the separation between the resonance frequencies. Relying on a power-like dependence like in Eq. (1), we conclude that for grains characterized by a single size a the band width is of the order of the resonance frequency itself.

One of our assumptions was smoothness of the grain boundaries. If the boundaries are rough, then a problem appears concerning an enhancement of energy losses observed in Ref. [47]. The giant electrical field enhancement leads to increasing non-linear effects. The problems needs a special investigation and are out of the scope of this work.

Appendix 1: Adiabatic approximation for quasi-plane gap

Consider dielectric gap between two bulk metal bodies. It is known that the surface plasmon wavenumber β in the gap is $2/d|\varepsilon|$ for ideally plane gap, where d is the thickness of the gap and ε is the ratio the dielectric constants ε_m and ε_d in the metal and the dielectric, respectively. The expression is valid in the quasi-static limit, when $|\varepsilon|^{3/2}d \ll \lambda/\sqrt{\varepsilon_d}$.

Let us derive wave equation for the surface plasmon, if the gap width slowly changes along the gap, so that adiabatic approximation for the wave propagation is applicable, when the wavelength is much less than the typical length where the gap width changes. Another derivation of the wave equation is given in Ref. [48].

Let us introduce Cartesian reference system and suppose for definiteness that the gap is symmetric in regards to OXY plane. Consider now a part of the gap, where the gap width $d(x, y)$ is slightly nonuniform, and thus, has a gradient $\nabla^\perp d$ (we denote $\nabla^\perp$ to be gradient operator in OXY plane). We locally approximate the boundaries of the gap by two planes which have mutual inclination angle $\gamma = |\nabla^\perp d|$. The adiabatic condition means that $\gamma\varepsilon \ll 1$.

The problem about surface plasmon wave propagation in a dielectric gap, whose boundaries are two intersecting planes, can be solved exactly. Let us direct OX axis along the gradient $\nabla^\perp d$, and introduce polar reference system ρ, φ in OXZ plane. The dielectric gap corresponds to angle $|\varphi| < \gamma/2$ and the gap width $d = \gamma\rho$ (see Fig. 2). The solution for the quasi-electrostatic equation $\mathrm{div}(\varepsilon(\mathbf{r})\,\mathrm{grad}\Phi) = 0$ can be written as $A(\rho, y)\sinh((2\varphi/\gamma)/\varepsilon)$ inside the gap (outside the gap at $\varphi > 0$ the solution is $A(\rho, y)\exp(-(2\varphi/\gamma)/\varepsilon)/\varepsilon)$. Wave equation on $A(\rho, y)$ reads $(\rho^{-1}\partial_\rho\rho\partial_\rho + \partial_y^2 + \beta^2)A = 0$, where local wavenumber $\beta = -2/\varepsilon d$. The equation can be rewritten in the form

$$((\nabla^\perp)^2 + \beta^2)(\beta^{-3/2}E_z) = 0. \qquad (39)$$

In (39) we dropped high corrections in $\nabla^\perp d$ that is correct in adiabatic limit when the surface plasmon wavelength in
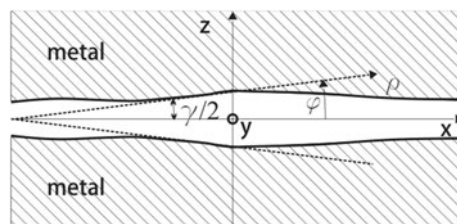

Fig. 2 Dielectric gap with slightly varying width

the direction of the gap alternation $\nabla^\perp d$ is much less than the typical length were the gap width changes. It is worth to mention that WKB approximation for wave equation (39) is applicable at the same condition as the equation was obtained.

The dependence of the electric field enhancement factor G (12) on the resonance number n can be obtained from investigation of the electric field spatial structure based on the developed theory of surface plasmon mode in quasi-planar gap. Let us assume the number n of the mode to be large. It is applicable adiabatic approximation to describe the surface plasmon mode inside the gap in the case. It looks like

$$\left(\frac{1}{\rho}\partial_\rho\rho\partial_\rho + \beta^2\right)\frac{E_z}{\beta^{3/2}} = 0, \quad \beta = -\frac{(\varepsilon\delta)^{-1}}{1 + \rho^2/h^2}. \tag{40}$$

in cylindrical coordinates. Solution at $\rho \lesssim h$ is $E_z \propto J_0(\rho/(|\varepsilon|\delta))$, where J_0 is Bessel function of zero order. To continue the solution into region $\rho \gtrsim h$, it is useful to rewrite Eq. (40) as

$$(\partial_\rho^2 + \beta_\rho^2)(\sqrt{\rho}E_z/\beta^{3/2}) = 0$$

where $\beta_\rho^2 = \beta^2 - 1/(4\rho^2)$, and use the WKB approximation to solve the equation. The WKB approximation is applicable between the turning points, when $\rho_s < \rho < \rho_c$. The turning points are determined by equating wavenumber β_ρ to zero, thus, $\rho_s = |\varepsilon|\delta/2 \sim h/n$ and $\rho_c = 2h^2/(|\varepsilon|\delta) \sim nh$. The solution for the electric field profile between the points is $E_z \propto \cos\left(\int^\rho \beta(\rho')\mathrm{d}\rho'\right)/(\beta\sqrt{\rho})$, since β_ρ is close to β in the region. Note that the integral under the cosine converges at $\rho \sim h$ that validates the previous evaluation (8). At $\rho \lesssim h$ the wavenumber is constant and E_z decays as $1/\sqrt{\rho}$, that corresponds to previously obtained solution in terms of Bessel function. The main part of Ohmic dissipation occurs in the region, it can be estimated as $I_Q \sim \omega\varepsilon''(E_c/n\varepsilon)^2(\sqrt{a\delta})^3$, that coincides with evaluation (11) for first mode. At $h < \rho < nh$, the wavenumber decreases as $1/\rho^2$ and the electric field decays as $1/\rho^{5/2}$. Although the filed decreases quite rapidly in the region, the main part of surface charge is accumulated on the scales. The value of the charge is determined by the last region with constant sing of E_z before the turning point ρ_c. The width of the region is quite large, $\Delta\rho \sim nh$, thus, the surface charge accumulated in the region is $\sim E_c a\delta/n$. At larger distances $\rho > \rho_c$, the adiabatic approximation is not applicable. The region corresponds to static limit, where potential difference between the surfaces does not depend on distance from the axis of the system. Thus, evaluation (10) looks now as $E_c/n \sim (d/a^2\delta)\ln(a/\delta)$. This means that the enhancement factor G obtains additional factor $1/n$ for modes with $n > 1$.

Appendix 2: Recurrence equation and electric field calculation between two spherical grains

The basis of eigen functions for Laplace operator can be chosen as follows in bispherical reference system:

$$\phi_{\alpha,m\pm} = \sqrt{\cosh\xi - \mu}\exp(\pm(\alpha + \tfrac{1}{2})\xi)\, P_\alpha^{|m|}(\mu)e^{im\varphi}, \tag{41}$$

where $P_\alpha^{|m|}$ is Legendre associated polynomial, $\alpha \geq |m|$ and $\mu = \cos\eta$. The recurrence equation (23) arises because of the boundary condition (4) and the normal derivative meshes the neighbouring harmonics. We used [Eq. 14.10.3, 42] when derivating the coefficients in the recurrence equation (23), which are

$$\begin{aligned}
X_{\alpha,m}^\pm &= -\left(\alpha + \tfrac{1}{2} \pm (m + \tfrac{1}{2})\right) \\
&\quad \times \left\{\cosh\left[(\alpha + \tfrac{1}{2} \pm 1)\xi_0)\right] + \varepsilon\sinh\left[(\alpha + \tfrac{1}{2} \pm 1)\xi_0\right]\right\}, \\
X_{\alpha,m} &= \varepsilon\left[e^{-\xi_0} + 2\alpha\cosh\xi_0\right]\sinh\left[(\alpha + \tfrac{1}{2})\xi_0\right] \\
&\quad + \cosh\left[(\alpha + \tfrac{3}{2})\xi_0\right] + 2\alpha\cosh\xi_0\cosh\left[(\alpha + \tfrac{1}{2})\xi_0\right],
\end{aligned} \tag{42}$$

$$\begin{aligned}
D_\alpha &= -\sqrt{2}aE_z^{\text{ext}}\sinh\xi_0(\varepsilon - 1) \\
&\quad \times \exp\left[-(\alpha + \tfrac{1}{2})\xi_0\right]\left[\alpha e^{\xi_0} - (\alpha + 1)e^{-\xi_0}\right].
\end{aligned} \tag{43}$$

The condition $\xi_0 \ll 1$ allows us to pass in recurrence equations (23) to continues limit far from special points. On the way, one obtains a linear differential equation of the second-order valid at $|\alpha - \alpha_\varepsilon| \gg 1$. The coefficients in the differential equation

$$\left(C_2^{|m|}\partial_\alpha^2 + C_1^{|m|}\partial_\alpha + C_0^{|m|}\right)B^m(\alpha) = D(\alpha)\delta^{m0} \tag{44}$$

are set by equations $C_2^{|m|}(\alpha) = (X_{\alpha,m}^+ + X_{\alpha,m}^-)/2, C_1^{|m|}(\alpha) = X_{\alpha,m}^+ - X_{\alpha,m}^-, C_0^{|m|}(\alpha) = X_{\alpha,m} - (X_{\alpha,m}^+ + X_{\alpha,m}^-)$. We consider mainly the axial symmetric modes, which correspond to $m = 0$. Equation (44) looks like

$$\left(\alpha(\alpha - \alpha_\varepsilon)\partial_\alpha^2 + (3\alpha - \alpha_\varepsilon)\partial_\alpha + 1\right)B = \sqrt{2}E_z^{\text{ext}}a \tag{45}$$

in the region $\alpha \ll 1/\xi_0$. Two linear independent solution of homogeneous version of Eq. 45) are

$$1/(\alpha - \alpha_\varepsilon), \quad \ln(\alpha/\alpha_\varepsilon)/(\alpha_\varepsilon - \alpha), \tag{46}$$

where the first one is B_α^{hom} introduced in Sect. 3.2. Partial solution of full equation (45) is $B = \sqrt{2}E_z^{\text{ext}}a$ [compare with (27)]. It is convenient to pass to variable $u = \alpha\xi_0$ in the limit $(\alpha - \alpha_\varepsilon) \gg 1$, after what the differential equation on B takes the form

$$\begin{aligned}
\left(u\sinh u\,\partial_u^2 + (2u\cosh u + \sinh u)\partial_u + e^u\right)B \\
= \sqrt{2}E_z^{\text{ext}}a\,e^{-u}(1 - 2u).
\end{aligned} \tag{47}$$

Two linear independent solutions of homogeneous version of (47) are

$$\frac{2/\xi_0}{e^{2u}-1}, \quad \frac{1}{e^{2u}-1}\int_1^u \frac{e^{2u'}}{u'}\,\mathrm{d}u'. \tag{48}$$

These solutions are continuation of solutions (46) correspondingly. The first one decreases exponentially, whereas the second one decreases only as $1/\alpha$ at large $\alpha \gg 1/\xi_0$. Thus, one should demand that the solution for expansion coefficient B_α should contain only the first solution in (46, 48) such that expression (24) should be satisfied. Partial solution of (47) is $2\sqrt{2}E_z^{\mathrm{ext}}au/(e^{2u}-1)$ [compare with (27)]. Let us implement matching of solutions of (45) and (47) using condition $\int_1^\infty B\mathrm{d}\alpha = 0$ which is the continuous analog of (24). As a result, we obtain

$$B = -\sqrt{2}E_z^{\mathrm{ext}}a\begin{cases} 1 - b/(\xi_0(\alpha - \alpha_\varepsilon)), & \alpha \ll 1/\xi_0 \\ 2(u-b)/(e^{2u}-1), & \alpha \gg \alpha_\varepsilon \end{cases} \tag{49}$$

where $b = \pi^2/(12\ln(1/\xi_0))$.

Finally, the electric field z-component in the plane $z = 0$ is expressed through expansion coefficients B_α as follows

$$E_z(\rho) = E_z^{\mathrm{ext}}\left[1 + \frac{\sqrt{a}}{\sqrt{\delta}}(1-\mu)^{3/2}\sum_{\alpha=0}^{\infty}(2\alpha+1)B_\alpha P_\alpha(\mu)\right]. \tag{50}$$

References

1. U. Kreibig, M. Vollmer, it Optical Properties of Metal Clusters, vol. 25 of Springer Series in Materials Science (Springer, Berlin, 1995)
2. A.K. Sarychev, V.M. Shalaev, Electrodynamics of metamaterials (World Scientific Publishing Company, Singapore, 2007)
3. C.F. Bohren, D.R. Huffman, Absorption and scattering of light by small particles. (Wiley, New York, 1983)
4. J. Berthelot, A. Bouhelier, C. Huang, J. Margueritat, G.C. des Francs, E. Finot, J.C. Weeber, A. Dereux, S. Kostcheev, H.I.E. Ahrach, A.L. Baudrion, J. Plain, R. Bachelot, P. Royer, G.P. Wiederrecht, Tuning of an optical dimer nanoantenna by electrically controlling its load impedance. Nano Lett. 9, 3914–21 (2009)
5. R.M. Bakker, H.K. Yuan, Z. Liu, V.P. Drachev, A.V. Kildishev, V.M. Shalaev, R.H. Pedersen, S. Gresillon, A. Boltasseva, Enhanced localized fluorescence in plasmonic nanoantennae. Appl. Phys. Lett. 92, 043101 (2008)
6. M.H.C.J. Zhang, Y. Fu, J. R. Lakowicz, Metal-enhanced single-molecule fluorescence on silver particle monomer and dimer: coupling effect between metal particles. Nano Lett. 7, 2101 (2007)
7. P.K. Jain, W. Huang, M. A. El-Sayed, On the universal scaling behavior of the distance decay of plasmon coupling in metal nanoparticle pairs: A plasmon ruler equation. Nano Lett. 7, 2080–2088 (2007)
8. D. Bloemendal, P. Ghenuche, R. Quidant, I. G. Cormack, P. Loza-Alvarez, G. Badenes, Local field spectroscopy of metal dimers by tpl microscopy. Plasmonics 1, 41–44 (2006)
9. W. Rechberger, A. Hohenau, A. Leitner, J. Krenn, B. Lamprecht, F. Aussenegg, Optical properties of two interacting gold nanoparticles. Opt. Commun. 220, 137–141 (2003)
10. K.-H. Su, Q.-H. Wei, X. Zhang, J.J. Mock, D.R. Smith, S. Schultz, Interparticle coupling effects on plasmon resonances of nanogold particles. Nano Lett. 3, 1087–1090 (2003)
11. Y. Chu, M.G. Banaee, K.B. Crozier, Double-resonance plasmon substrates for surface-enhanced raman scattering with enhancement at excitation and stokes frequencies. ACS Nano 4, 2804 (2010)
12. Y. Cheng, M. Wang, G. Borghs, H. Chen, Gold nanoparticle dimers for plasmon sensing. Langmuir 27, 7884 (2011)
13. G. Haran, Accounts of chemical research Single-molecule Raman spectroscopy: a probe of surface dynamics and plasmonic fields 43, 1135–43 (2010)
14. K. Kneipp, M. Moskovits, H. Kneipp, eds., Surface-Enhances Raman Scattering vol. 103 of Topics in Applied Physics (Springer, Berlin, 2006)
15. J. Clarkson, J. Winans, P. Facuhet, On the scaling behavior of dipole and quadrupole modes in coupled plasmonic nanoparticle pairs. Opt. Mater. Exp.1, 970 (2011)
16. V. Amendola, O. M. Bakr, F. Stellacci, A study of the surface plasmon resonance of silver nanoparticles by the discrete dipole approximation method: Effect of shape, size, structure, and assembly. Plasmonics 5, 85–97 (2010)
17. I. Romero, J. Aizpurua, G.W. Bryant, F.J.G. De Abajo, Plasmons in nearly touching metallic nanoparticles: singular response in the limit of touching dimers. Opt. Exp. 14, 9988–99 (2006)
18. K. Seal, D. A. Genov, A.K. Sarychev, H. Noh, V.M. Shalaev, Z.C. Ying, X. Zhang, H. Cao, Coexistence of localized and delocalized surface plasmon modes in percolating metal films. Phys. Rev. Lett. 97, 206103 (2006)
19. K. Seal, M. A. Nelson, Z.C. Ying, D. A. Genov, A.K. Sarychev, V.M. Shalaev, Growth, morphology, and optical and electrical properties of semicontinuous metallic films. Phys. Rev. B 67, 035318 (2003)
20. D. Genov, V. Shalaev, A. Sarychev, Surface plasmon excitation and correlation-induced localization-delocalization transition in semicontinuous metal films. Phys. Rev. B 72, 113102 (2005)
21. M.K. Hossain, Y. Kitahama, V. Biju, T. Itoh, T. Kaneko, Y. Ozaki, Surface plasmon excitation and surface-enhanced raman scattering using two-dimensional close-packed gold nanoparticles. J. Phys. Chem. C 113, 11689–11694 (2009)
22. J. Zeng, J. Huang, W. Lu, X. Wang, B. Wang, S. Zhang, J. Hou, Necklace-like noble-metal hollow nanoparticle chains: Synthesis and tunable optical properties. Adv. Mater. 19, 2172–2176 (2007)
23. P.B. Johnson, R.W. Christy, Optical constants of the noble metals. Phys. Rev. B 6, 4370 (1972)
24. A.D. Boardman, B.V. Paranjape, The optical surface modes of metal spheres. J. Phys. F: Metal Phys. 7, 1935 (1977)
25. V. Lebedev, S. Vergeles, P. Vorobev, Giant enhancement of electric field between two close metallic grains due to plasmonic resonance. Opt. Lett. 35, 640 (2010)
26. V.V. Klimov, D.V. Guzatov, Strongly localized plasmon oscillations in a cluster of two metallic nanospheres and their influence on spontaneous emission of an atom. Phys. Rev. B 75, 024303 (2007)
27. A.J. Hallock, P.L. Redmond, L.E. Brus, Optical forces between metallic particles. PNAS 102, 1280–1284 (2005)
28. R. Ruppin, Optical absorption of two spheres. J. Phys. Soc. Jpn. 58, 1446 (1989)
29. R. Ruppin, Surface modes of two spheres. Phys. Rev. B 26, 3440–3444 (1982)
30. P.K. Aravind, A. Nitzan, H. Metiu, Surf. Sci. 110, 189–204 (1981)

31. A. Goyette, A. Navon, Two dielectric spheres in an electric field. Phys. Rev. B **13**, 4320 (1976)

32. V. Babicheva, S. Vergeles, P. Vorobev, S. Burger, Localized surface plasmon modes in a system of two interacting metallic cylinders. J. Opt. Soc. Am. B **29**, 1263–1269 (2012)

33. S.B. Ogale, V.N. Bhoraskar, P.V. Panat, Surface plasmon dispersion relation for spherical metal particles. Pramana **11**, 135–144 (1978)

34. P. Nordlander, C. Oubre, E. Prodan, K. Li, M.I. Stokman, Plasmon hybridization in nanoparticle dimers. Nano Lett. **4**, 899–903 (2004)

35. G. Sun, J. Khurgin, A. Bratkovsky, Coupled-mode theory of field enhancement in complex metal nanostructures. Phys. Rev. B **84**, 045415 (2011)

36. I.P. Kaminow, W.L. Mammel, H.P. Weber, Metal-clad optical waveguides: analytical and experimantal study. Appl. Opt. **13**, 396–405 (1974)

37. M.H. Davis, Two charged spherical conductors in a uniform electric field: forces and field strength. Q. J. Mech. Appl. Math. **17**, 499–511 (1964)

38. P.M. Morse, H. Feshbach, Methods of Theoretical Physics. Part I (McGraw-Hill Book Company, inc. & Kogakusha company ltd., 1953)

39. J.Q. Feng, Electrostatic interaction between two charged dielectric spheres in contact. Phys. Rev. E **62**, 2891 (2000)

40. I.E. Mazets, Polarization of two close metal spheres in an external homogeneous electric field. J. Tech. Phys. **45**, 1238–1240 (2000)

41. E.C. Le Ru, C. Galloway, P.G. Etchegoin, Phys. Chem. Chem. Phys. **8**, 3083–3087 (2006)

42. F.W. J. Olver, D.W. Lozier, R.F. Boisvert, and C.W. Clark, NIST Handbook of Mathematical Functions (NIST National Institute of Standards and Technology & Cambridge University Press, 2010)

43. A.P. Prudnikov, Y.A. Brychkov, and O.I. Marichev, Integrals and series. Vol. 3. Spesial functions. Additional chapters. (FIZ-MATLIT, 2003), 2nd ed.

44. V.M. Shalaev, Nonlinear optics of random media, fractal composites and metal-dielectric films vol. 158 of Springer tracts in modern physics (Springer, Berlin, 2000)

45. V.M. Shalaev, Optical Properties of Nanostructured Random Media (Springer, Berlin, 2002)

46. Z. Liu, A. Boltasseva, R. Pedersen, R.M. Bakker, A.V. Kildishev, V.P. Drachev, V.M. Shalaev, Plasmonic nanoantenna arrays for the visible. Metamaterials **2**, 45–51 (2008)

47. V.P. Drachev, U.K. Chettiar, A.V. Kildishev, H.-K. Yuan, W. Cai, V.M. Shalaev, The ag dielectric function in plasmonic metamaterials. Opt. Exp. **16**, 1186–1195 (2008)

48. D. A. Smirnova, A. I. Smirnovı, A. A. Zharov, Two-dimensional plasmonic eigenmode nanolocalization in an inhomogeneous metal-dielectric-metal slot waveguide. JETP Lett. 96, 262–267 (2012)